System efficiency of packed bed TES with radial flow vs. axial flow – Influence of aspect ratio

Matthew E. Skuntz, Rachel Elander, Mohammad Al Azawii, Pablo Bueno, Ryan Anderson

System efficiency of packed bed TES with radial flow vs. axial flow – influence of aspect ratio

Matthew E. Skuntz[1], Rachel Elander[2], Mohammad Al Azawii[3], Pablo Bueno[4], Ryan Anderson[2]

[1] Mechanical and Industrial Engineering, Montana State University, Bozeman MT 59718, United States

[2] Chemical and Biological Engineering, Montana State University, Bozeman MT 59718, United States

[3] Department of Mechanical Engineering, University of Misan, Amarah, Misan 62001, Iraq

[4] Southwest Research Institute, Mechanical Engineering Division, San Antonio, TX 78238, United States

Abstract

This paper compares the net system efficiency, including thermal efficiency and pressure drop effects, of radial versus axial flow packed beds for thermal energy storage. The traditional packed bed system is a cylindrical geometry where fluid flows axially from one end to another. However, issues of thermal stratification and high-pressure drop have led to recent studies on radial flow systems. One potential benefit is the reduced pressure drop in a radial flow system. This paper compares the performance of radial flow and axial flow systems at a range of aspect ratios (AR = H/D_{bed}) from 0.21 to 1.92 using a numerical model where the storage volume is held constant in all cases. When the radial flow bed is at a low aspect ratio (short/wide), the thermal front is improved but the pressure drop is high. At a high aspect ratio, the velocity is reduced in radial flow, leading to decreased pressure drop but an increased spreads in the thermal front that lowers thermal efficiency. The opposite trends are noted in axial flow. Thermal efficiencies of 83-91% were noted for radial flow, while they ranged from 85-94% in axial flow. Net efficiencies including pressure drop ranged from 74-82% for radial flow and 80-87% for axial flow. In both systems, a peak net efficiency was noted between the highest and lowest aspect ratio. While some aspect ratios with radial flow outperform axial flow from a net efficiency perspective, the results show that the highest net efficiency from axial flow is higher than that from radial flow. Overall, this paper highlights the importance of innovative TES designs and their potential to improve energy efficiency.

Keywords: Packed bed thermal energy storage; radial flow; aspect ratio; exergy efficiency

1 Introduction

Many types of packed bed thermal energy storage systems have been studied [1], and Trevisan et al. [2, 3] recently highlighted current approaches to packed bed thermal energy storage (PBTES). The traditional packed bed is a container, commonly a cylinder, where fluid moves axially from one end to the other. Within this geometry, many variables have been studied, such as aspect ratio, flow rate, temperature, storage materials, phase change materials (PCMs) vs. sensible storage media, heat transfer fluids etc. In general, lab experimental tests are smaller and larger systems are demonstrated numerically. Not all groups present the same metrics, so direct comparisons are not always possible. However, general trends emerge. High thermal stratification is possible with exergetic efficiencies over 95%, particularly when losses to the environment are minimized/eliminated [4]. However, thermal stratification issues remain a practical challenge [5]. Several studies that investigated traditional axial flow in thermal energy storage (TES) packed bed systems were discussed in review papers [1, 6, 7].

Variations from the traditional bed include: a) truncated conical packed beds [8] b) unconstrained packed bed [9, 10]; c) layered parallel packed bed TES [11], axial sliding flow [12], and axial pipe injections [13]. Details on many of these configurations are presented in ref. [3]. Each new design aims to solve some problem compared to the baseline axial flow configuration. For instance, the conical configuration was proposed to limit ratcheting effects. This geometry can have high efficiency with reported energetic and exergetic efficiencies over 98% [14]. However, this result was achieved in part with 60 cm of insulation (100 MW_{th} numerical model with H = 25 m, R_{top} = 49.19 m, R_{bottom} = 45.29 m). In general in all TES configurations, the goal is to have a sharp thermocline with minimal heat losses, low pressure drop, and no temperature gradient in the storage particles.

Recent work has studied radial flow systems instead of the traditional axial flow e.g., references [3,15-17]. In radial flow systems, flow first emerges from the center of the bed via internal piping. As it flows outwardly, the velocity decreases, which can lead to lower pressure drop. Figure 1 shows arrows for the flow direction of charge and discharge via radial flow at aspect ratios utilized in the present study. Here, the aspect ratio is defined as AR = H/D_{bed}, where a short and wide bed is a low aspect ratio system. The solid line represents charging, with the flow from the center outward, while the dashed line represents discharging with cold fluid entering from the outer edge and exiting in the center.

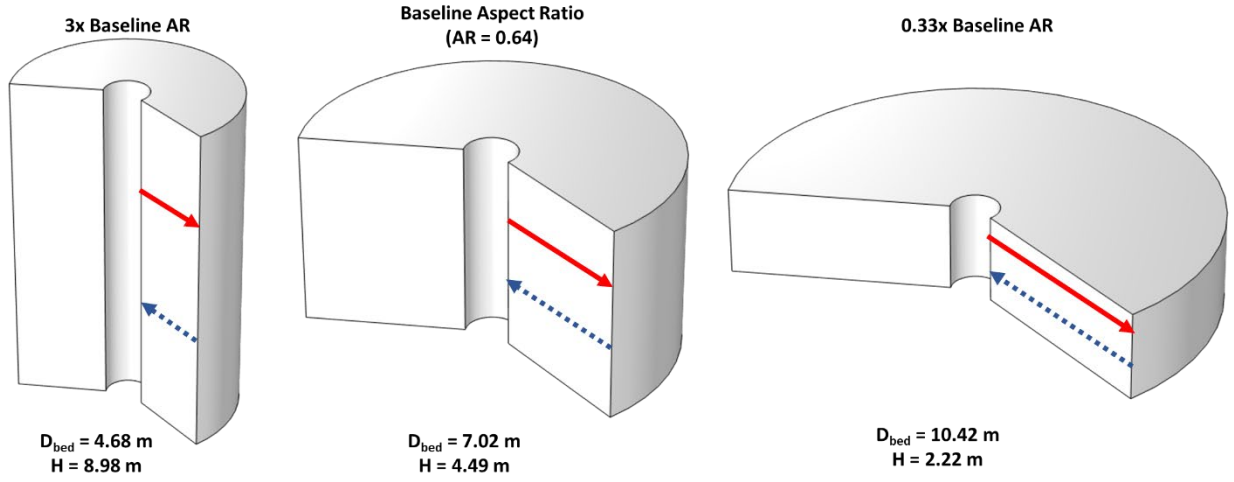

Figure 1. Radial flow concept with specific range of aspect ratios and dimensions studied numerically for axial and radial flow

In previous initial efforts with radial flow [15], a plastic central pipe was drilled to provide perforations/a flow path from the pipe. Internal baffles ensured fluid went from the center to the wall. The flow could then flow axially toward the 'traditional' outlet. This could be considered a 'partial' radial system as there was still an axial component to the flow in the bed. Trevisan's work [3] provided one of the first larger lab-scale experimental tests of the radial flow concept, with a charge inlet temperature at 700°C and a discharge inlet temperature of 25°C. In charge, flow entered the center piping, which contained a metallic mesh. Fluid then moved through the bed to deposit heat and exits via an annulus. There is an element of self-insulation as the bed does not directly touch the vessel wall or other internal insulation. This system showed a maximum thermal efficiency of 71.8% despite low thermal losses to the ambient; the main issue was thermocline spread. Short cycles (30 min) decreased charge efficiency but increased discharge efficiency, which can lead to ~70% thermal efficiency [16]. McTigue and White show that while radial flow can perform similarly to axial flow in terms of thermal efficiency, it does so at the

expense of large volumes and thus more cost [17]. Another innovative radial system, THERMS, was proposed by Ho [18].

In this paper, radial flow is compared to axial flow at nine aspect ratios. In all cases, the inlet temperature to charge the packed bed is 600°C, and the storage volume is kept constant. Temperature profiles are presented for the thermoclines in the bed along with the recovery temperature during the discharge cycle. The results are analyzed in terms of overall thermal efficiency, parasitic power losses from the pressure drop, and an overall system efficiency that considers both thermal and hydraulic effects during a full charge-discharge cycle.

2 Numerical Model

The packed bed TES design is based on a commercial-scale unit outlined in ref. [2]. The flow rate is 34.65 kg/s with a constant storage volume of 232 m^3 in all configurations. The charge temperature is 600°C with air, and the recovery inlet is air at 20°C. The outlet pressure in charging and discharging is set to 1 atm. These conditions represent a 22.5 MW storage bed. To compare radial and axial flow configurations, each bed is charged and discharged for 8.75 hours (17.5 hours for a full cycle). The models use an axisymmetric configuration where the location r = 0 is a symmetry plane. The general geometry for radial flow is shown in Figure 1. The gap from the symmetry plane to the packed bed is where a central pipe would be located. However, additional analysis by our group (results not presented here) has shown that even flow is possible into the bed when considering a large central and receiving pipe. Thus, flow in these pipes was removed and flow only goes through the packed bed. In the radial configuration, D_{bed} is the difference between the outer and the inner diameter (only the packing domain is considered in the bed diameter). The inner diameter of the bed is 1.174 m. In axial flow, no peripheral piping is considered, and flow is vertical with heated flow entering from the top in charging and from the bottom in discharging. As the central pipe is not needed in axial flow, the geometry is scaled to the same aspect ratios as radial flow, meaning the diameter and height differ between the radial and axial systems. All models assume adiabatic conditions as the goal is to compare baseline performance between the radial and axial design configurations. The baseline aspect ratio above was 0.64 (AR = H/D_{bed}), and a total of nine aspect ratios were considered. Other designs were based on a multiplier of the baseline aspect ratio (AR multiplier), which varied from 3x to 1/3x the baseline aspect ratio. The resulting aspect ratios, bed diameters, and heights for radial and axial flow are noted in Table 1. The highest, baseline, and lowest aspect ratios are shown in Figure 1.

Table 1. Nine designs all with constant volume but varying aspect ratio

	Radial		Axial		
AR Multiplier	**D_bed (m)**	**H (m)**	**D_bed (m)**	**H (m)**	**AR**
3x	4.68	8.98	5.36	10.29	1.92
2.5x	5.01	8.01	5.69	9.11	1.60
2x	5.44	6.97	6.13	7.85	1.28
1.5x	6.05	5.81	6.75	6.48	0.96
Baseline AR	**7.02**	**4.49**	**7.73**	**4.95**	**0.64**
0.67x	8.13	3.47	8.85	3.77	0.43
1/2x	9.01	2.88	9.74	3.12	0.32
0.4x	9.76	2.50	10.49	2.69	0.26

1/3x	10.42	2.22	11.15	2.38	0.21

The models treated the air as compressible, so the local velocity is calculated with changes in temperature and pressure. Air's density, viscosity, thermal conductivity, and heat capacity vary with temperature via the solver's embedded database. The models do not consider temperature dependent thermophysical properties of the storage media. Bed properties include a porosity of 0.385, particle diameter of 6 mm, thermal conductivity of 27 W/m*K, density of 3,975 kg/m^3, and heat capacity of 900 J/kg*K. Mass and momentum conservation are shown in Equations 1 and 2. The viscous and inertial terms through the packing are in Equations 3 and 4 based on coefficients in the Ergun equation. The single-phase energy equation shown in Equation 5 assumes a homogenous medium in the packed bed and uses effective (eff) volume-averaged properties (Equations 6 and 7). These equations were solved in COMSOL 5.6.

$$\nabla \cdot (\rho \boldsymbol{u}) = 0 \tag{1}$$

$$\frac{\rho}{\varepsilon_p}(\boldsymbol{u} \cdot \nabla)\frac{\boldsymbol{u}}{\varepsilon_p} = -\nabla p + \left(\frac{\mu}{\varepsilon_p}(\nabla \boldsymbol{u} + (\nabla \boldsymbol{u})^T)\right) - (\mu \kappa^{-1} + \beta \rho \boldsymbol{u})\boldsymbol{u} \tag{2}$$

$$\kappa = \frac{(d_p^2 \varepsilon_p^3)}{\left(150 \cdot \left(1 - \varepsilon_p\right)^2\right)} \tag{3}$$

$$\beta = \frac{1.75 \cdot \left(1 - \varepsilon_p\right)}{(d_p \varepsilon_p^3)} \tag{4}$$

$$(\rho \mathrm{C_p})_{\mathrm{eff}} \frac{\partial \mathrm{T}}{\partial \mathrm{t}} + (\rho \mathrm{C_p})_{\mathrm{f}} \boldsymbol{u} \cdot \nabla \mathrm{T} = \nabla \cdot \left(k_{eff} \nabla \mathrm{T}\right) \tag{5}$$

$$(\rho \mathrm{C_p})_{\mathrm{eff}} = \varepsilon \rho_{\mathrm{f}} \mathrm{C_{p,f}} + (1 - \varepsilon)\rho_{\mathrm{s}} \mathrm{C_{p,s}} \tag{6}$$

$$k_{eff} = \varepsilon k_f + (1 - \varepsilon)k_s \tag{7}$$

The thermal power (W) in recovery was calculated by:

$$ThermalPower_{rec.} = \dot{m} c_{p,air}\left(T_{rec.avg} - T_{low}\right) \tag{8}$$

while the parasitic power (W) from the pressure drop was calculated by:

$$PumpPower = \dot{m} * Work = \dot{m}\frac{P_{out,avg} - P_{in}}{\rho_{avg}} \tag{9}$$

The recovery temperature, pressure, and density vary with time at the outlet during discharge In Eqns. 8 and 9, these values were calculated from an average over the entire duration of the discharge period. The net recovery power was then defined as:

$$Net\ Power_{rec.} = ThermalPower_{rec.} - PumpPower \tag{10}$$

while the net efficiency was defined as:

$$Net\ Efficiency = \frac{Net\ Power_{rec.}}{Power_{charge}} \tag{11}$$

3 Results and Discussion

The results are analyzed in terms of energy efficiency based on the recovery temperature after a full cycle and the pressure drop. The overall thermal efficiency is based on the recovery temperature of the

discharge cycle, which is a function of the thermal front within the bed. The thermal front for radial and axial flow is shown in **Figure 2** at two aspect ratios at three times during charge (1 hr, 4.5 hrs, 8.75 hrs). The position is made dimensionless relative to the mass of the bed to clearly compare between the two configurations. In **Figure 2**a, the aspect ratio is at the baseline. In the earlier time steps (1 hr, 4.5 hrs), the thermal fronts are similar for radial and axial flow configurations. However, by the end of charge, the radial system's thermal front has spread more, evidenced by the higher temperature at the outlet. At 2x the baseline ratio, the axial system's thermal front is much sharper. As will be shown, these results lead to higher thermal efficiency for axial flow vs. radial flow at these aspect ratios.

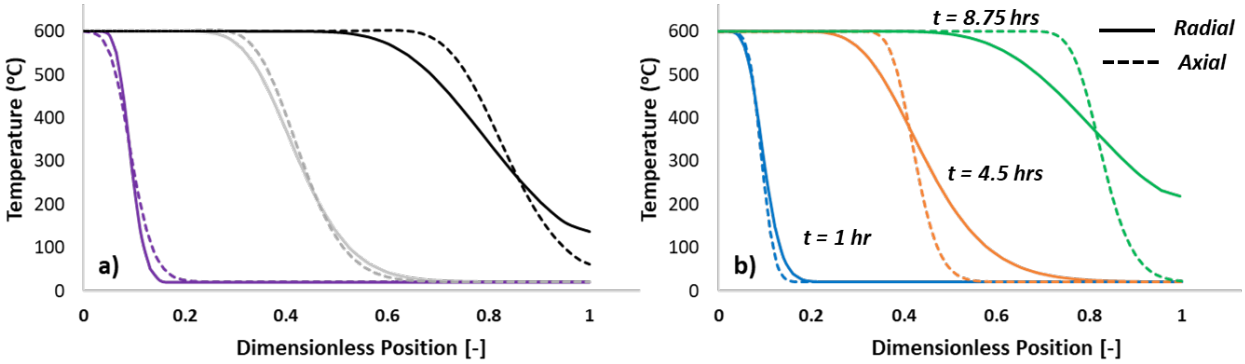

Figure 2. Bed temperature vs. dimensionless position for radial vs. axial flow at three times a) Baseline aspect ratio b) 2x AR

These results relate to the Peclet number (*Pe*), which is a ratio of diffusive to convective transport. In all cases, the thermal conductivity of the media and heat transfer fluid is constant. The velocities are noted in **Table 2**. Higher velocity lowers conduction effects relative to convective, causing sharper thermal fronts. Changing the aspect ratio changes the velocity and thus the magnitude of the convective transport. As the velocity increases, *Pe* increases, leading to a sharper thermal front. Thus, when the bed's aspect ratio is increased in axial flow, the diameter is lower and the velocity increases. This effect leads to a sharper front and overall higher efficiency. Conversely for radial flow, as the aspect ratio increases, the height increases (e.g., Figure 1 left). This change leads to a decrease in the velocity in the radial direction, which increases conduction effects relative to convective effects. The increase in conduction leads to a broader thermal front.

The resulting recovery temperature for radial flow is shown in Figure 3. As the aspect ratio decreases (wide, short), a higher recovery temperature is noted. These recovery profiles are consistent with the thermal front in the bed as explained above.

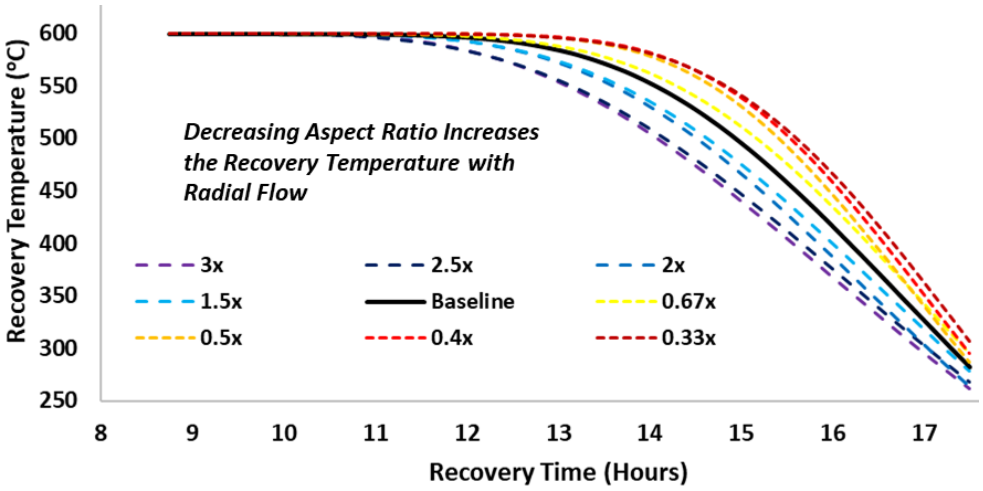

Figure 3. Recovery temperature at nine aspect ratios for radial flow

The resulting thermal efficiencies for radial and axial flow are seen in **Table 2**. For radial flow, these temperatures led to thermal energy efficiencies of 83-91%. For axial flow, the thermal efficiency ranged from 85-94%. As can be seen, for some aspect ratios, the thermal efficiency is higher in radial flow. This occurs when the aspect ratio is low. For radial flow, this means high velocity while for axial flow this means low velocity. For axial flow at 3x and 2.5x, the pressure drop is excessive, and these models did not converge. These high pressure drop results would be not practical in a real system. Further, considering the trends in net efficiency, these cases would be the lowest overall efficiency of any case considered.

Table 2. Inlet velocities, pressure drop, thermal efficiencies, and net system efficiency for radial vs. axial flow configurations at nine aspect ratios.

ARx	Radial ΔP (Pa)	Axial ΔP (Pa)	Rad. Thermal Eff. (%)	Ax. Thermal Eff. (%)	Radial Net Eff. (%)	Axial Net Eff. (%)
3x	4,725	NA	83.1	NA	81.4	NA
2.5x	5,854	NA	83.7	NA	81.5	NA
2x	8,321	49,433	85.2	94.3	82.2	79.7
1.5x	10,647	31,731	86.0	93.5	82.3	83.5
1x	16,918	16,370	87.6	92.4	81.8	86.9
0.67x	26,832	8,168	89.4	90.3	80.6	87.5
0.5x	37,165	4,972	89.9	88.3	78.2	86.6
0.4x	47,330	3,384	90.6	86.7	76.3	85.5
0.33x	57,522	2,471	91.0	84.9	74.3	84.1

The system-level (or net) efficiency includes hydraulic effects, i.e., the pressure drop through the bed leading to a parasitic power loss (Equation 10). These results are shown in **Figure 4**. The aspect ratios lead to opposite changes in pressure drop for radial and axial flow. For instance, at an AR multiplier of 2 (actual aspect ratio of 1.28), the radial flow bed is taller than it is wide, leading to a larger cross-sectional area for flow while the opposite is true for the axial bed.

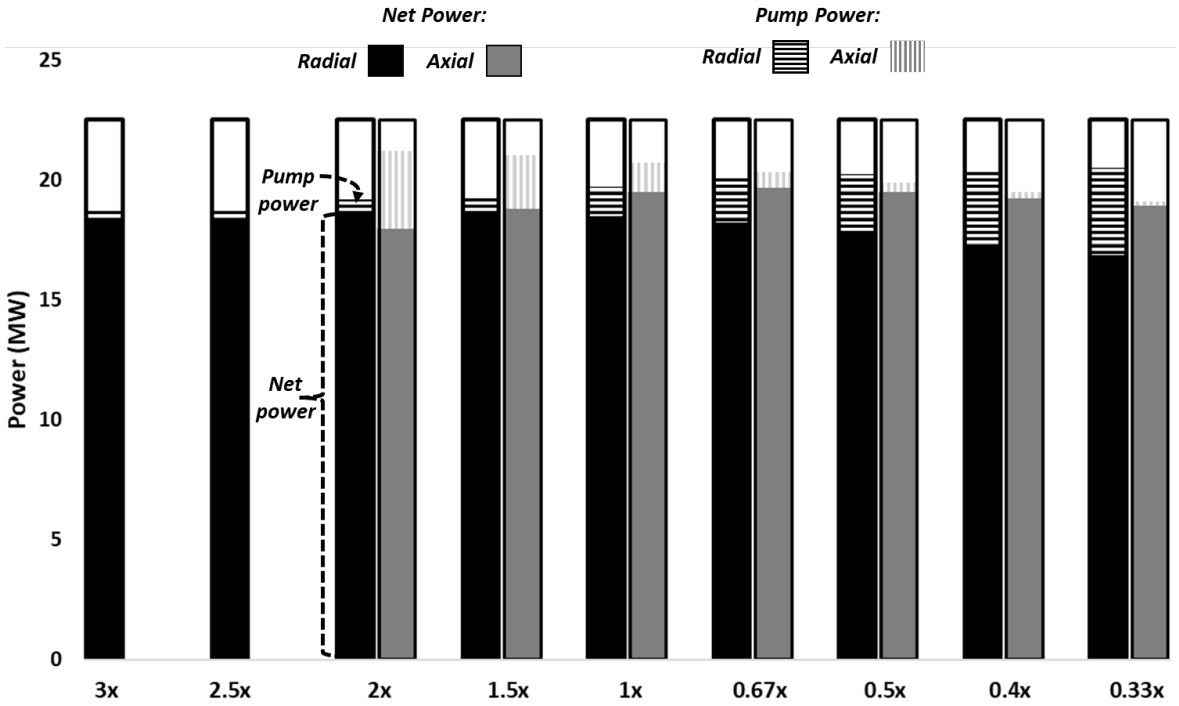

Figure 4. Net power and pump power for axial and radial configurations. The tallest area in all cases represents the designed power of 22.5 MW. The solid bars represent the net power for radial (black) and axial (configurations). The dashed areas represent the magnitude of the pumping power. The sum of the net power and pump power is the thermal power recovered after the cycle.

A more direct comparison of the pressure drop then is between radial at 2x and axial at 0.5x (or radial at 1.5x and axial at 0.67x etc.). When compared this way, radial flow had a lower pressure drop when the AR multiplier was less than 1 but a higher pressure drop when the AR multiplier was above 1 (actual aspect ratios from 0.64 and above). From a net-system perspective, there are some cases where the radial system outperforms axial, such as at 2x. In other cases though, the axial configuration is better. For the conditions of this study, the highest net efficiency from the axial configuration is higher than the highest net efficiency from the radial configuration.

Note, these results are for ideal performance based only on the packing in the bed (all peripherals etc. are neglected). This scope was intentional to focus directly on comparing the relative thermal and hydraulic merits of the two flow systems. One issue may be thermomechanical stresses induced by the temperature gradient in the radial direction; hotter particles near the center can expand more than neighboring particles, causing stress. Also, real systems would experience heat losses to the ambient environment, which will be a function of the specific choices made in the vessel design i.e., they vary between systems and thus heat losses are likely to be unique between the systems. Radial flow has been described as self- insulating since the outlet during charge, which does not have high temperature, is near the wall. Thus, heat losses can be minimized. However, for the same vessel size, more insulation could likely be added to an axial system to achieve similar insulation. These effects, and their relative economic impact, are beyond the scope of the present work. However, as noted by [17], the larger tanks can lead to higher cost in radial systems as well. This economic disadvantage would be compounded in pressurized systems.

4 Conclusions

This paper numerically analyzed radial flow vs. axial flow in terms of thermal performance and pressure drop. In radial and axial flow, the vessel represented a 22.5 MW storage unit with T_{hot} at 600°C. The aspect ratios ranged from 0.21 to 1.92 with a baseline design at 0.64.

1. In some cases, but not all, radial flow systems have lower pressure drops but a higher spread in the thermal front that lowers thermal efficiency. On the other hand, axial flow systems had a higher thermal efficiency but higher pressure drops.
2. Thermal efficiencies of 83-91% were noted for radial flow, while they ranged from 85-94% in axial flow. Net efficiencies including pressure drop ranged from 74-82% for radial flow and 80-87% for axial flow.
3. The highest net efficiency from axial flow is higher than that from radial flow, although some aspect ratios with radial flow outperform axial flow from a net efficiency perspective.

5 Nomenclature

β – inertial term in packed bed pressure drop
ε_p – packed bed porosity [-]
κ – viscous term in packed bed pressure drop
ρ – density [kg/m^3]
μ – viscosity [Pa.s]

c_P – heat capacity [J/(kg.K)]
D – diameter [m]
H – height [m]
k – thermal conductivity [W/(m.K)]
P – Pressure [Pa]
R – radius [m]
T – temperature [K]
t – time [s]
$\boldsymbol{u}$ – velocity vector [m/s]
V – volume [m^3]

AR – aspect ratio [-]
PBTES – packed bed thermal energy storage
PCM – phase change material
TES – thermal energy storage
eff – effective property
rec. – recovery
f - fluid
s - solid

6 Acknowledgements

This material is based upon work supported by the U.S. Department of Energy's Office of Energy Efficiency and Renewable Energy (EERE) under the Solar Energy Technology Office Award Number DE-EE0009384. This report was prepared as an account of work sponsored by an agency of the United States Government. Neither the United States Government nor any agency thereof, nor any of their employees, makes any warranty, express or implied, or assumes any legal liability or responsibility for the accuracy, completeness, or usefulness of any information, apparatus, product, or process disclosed, or represents that its use would not infringe privately owned rights. Reference herein to any specific commercial product, process, or service by trade name, trademark, manufacturer, or otherwise does not necessarily constitute or imply its endorsement, recommendation, or favoring by the United States Government or any agency thereof. The views and opinions of authors expressed herein do not necessarily state or reflect those of the United States Government or any agency thereof.

References

1. Gautam, A. and R. Saini, *A review on technical, applications and economic aspect of packed bed solar thermal energy storage system.* Journal of Energy Storage, 2020. **27**: p. 101046.
2. Trevisan, S., et al. *Initial design of a radial-flow high temperature thermal energy storage concept for air-driven CSP systems*. in *AIP Conference Proceedings*. 2019. AIP Publishing LLC.
3. Trevisan, S., et al., *Experimental evaluation of an innovative radial-flow high-temperature packed bed thermal energy storage.* Applied Energy, 2022. **311**: p. 118672.
4. Bindra, H., et al., *Thermal analysis and exergy evaluation of packed bed thermal storage systems.* Applied Thermal Engineering, 2013. **52**(2): p. 255-263.
5. Palacios, A., et al., *Thermal energy storage technologies for concentrated solar power–A review from a materials perspective.* Renewable Energy, 2020. **156**: p. 1244-1265.
6. Esence, T., et al., *A review on experience feedback and numerical modeling of packed-bed thermal energy storage systems.* Solar Energy, 2017. **153**: p. 628-654.
7. Gautam, A. and R. Saini, *A review on sensible heat based packed bed solar thermal energy storage system for low temperature applications.* Solar energy, 2020. **207**: p. 937-956.
8. Zanganeh, G., et al., *Packed-bed thermal storage for concentrated solar power – Pilot-scale demonstration and industrial-scale design.* Solar Energy, 2012. **86**(10): p. 3084-3098.
9. P, G., *South African provisional patent application. 2014/03555.* 2014.
10. Allen, K., et al. *Rock bed thermal storage: Concepts and costs*. in *AIP Conference Proceedings*. 2016. AIP Publishing LLC.
11. Schlipf, D., et al. *First operational results of a high temperature energy storage with packed bed and integration potential in CSP plants*. in *AIP Conference Proceedings*. 2017. AIP Publishing LLC.
12. Bindra, H., P. Bueno, and J.F. Morris, *Sliding flow method for exergetically efficient packed bed thermal storage.* Applied Thermal Engineering, 2014. **64**(1-2): p. 201-208.
13. Al-Azawii, M.M.S., et al., *Experimental study of layered thermal energy storage in an air-alumina packed bed using axial pipe injections.* Applied Energy, 2019. **249**: p. 409-422.
14. Singh, S., et al., *Investigation on transient performance of a large-scale packed-bed thermal energy storage.* Applied Energy, 2019. **239**: p. 1114-1129.
15. Al-Azawii, M.M., et al., *Experimental study of thermal behavior during charging in a thermal energy storage packed bed using radial pipe injection.* Applied Thermal Engineering, 2020. **180**: p. 115804.
16. Trevisan, S., et al., *Experimental evaluation of a high-temperature radial-flow packed bed thermal energy storage under dynamic mass flow rate.* Journal of Energy Storage, 2022. **54**: p. 105236.

17. McTigue, J.D. and A.J. White, *A comparison of radial-flow and axial-flow packed beds for thermal energy storage.* Applied Energy, 2018. **227**(C): p. 533-541.
18. Ho, C.K. and W. Gerstle. *Terrestrial Heat Repository for Months of Storage (THERMS): A Novel Radial Thermocline System*. in *Energy Sustainability*. 2021. American Society of Mechanical Engineers.